

A Nonparametric Approach for Noisy Point Data Preprocessing

Yongjian Xi^a, Ye Duan^{a*}, Hongkai Zhao^b

^a University of Missouri, Columbia, MO 65211, USA

^b University of California at Irvine, Irvine, CA, 92710, USA

*duanye@missouri.edu

Abstract

3D point data acquired from laser scan or stereo vision can be quite noisy. A preprocessing step is often needed before a surface reconstruction algorithm can be applied. In this paper, we propose a nonparametric approach for noisy point data preprocessing. In particular, we proposed an anisotropic kernel based nonparametric density estimation method for outlier removal, and a hill-climbing line search approach for projecting data points onto the real surface boundary. Our approach is simple, robust and efficient. We demonstrate our method on both real and synthetic point datasets.

1. Introduction

Despite significant advancement in interactive shape modeling, creating realistic looking 3D models from scratch is still a very challenging task. Recent advancement in 3D shape acquisition systems such as laser range scanner, structural light system and stereo vision system have made direct 3D data acquisition feasible [1].

The obtained point dataset however can be quite noisy. Without preprocessing to deal with noisy data, parametric and/or variational formulations [10-21] are usually used. These methods generally composed of both a fitting term for the data and a regularization term for the reconstructed surface. Since all data points, even outliers, are treated equally and can affect the final reconstruction, these approaches will likely fail for highly noisy data.

Another type of algorithms is based on popular computational geometry algorithms such as Delaunay triangulations and Voronoi diagrams to construct triangulated surfaces [2, 3, 4, 5, 6]. For this kind of method, it is challenging to find the right connections among all data points in three and higher dimensions, especially for noisy data.

Recently, Medioni et al. proposed the tensor voting method [8], which is a nice feature extraction algorithm. By designing an appropriate voting procedure among all data points, a tensor field and an associated saliency field can be constructed. Coherent

geometric information can be extracted from the tensor field and the saliency field. However, tensor voting method is computationally very expensive.

In this paper, we propose a nonparametric approach for noisy point data preprocessing. In particular, we proposed an anisotropic kernel based nonparametric density estimation method for outlier removal, and a hill-climbing line search approach for projecting data points onto the real surface boundary. Our approach is simple, robust and efficient. We demonstrate our method on both real and synthetic point datasets.

2. Algorithm

2.1 Parzen-window based kernel density estimation

Points outside the object surface are outliers that have to be removed. Since the real object surface is unknown, it is hard to specify a general criterion to detect outliers. In this paper, we propose to employ parzen-window based nonparametric density estimation method for outlier removal.

Parzen window based kernel density estimation is the most popular nonparametric density estimation method. In order to make the paper self-contained, we will briefly review the Parzen window method in the following. For a complete description, please refer to the book by Duda et al. [9].

Given n data points x_i , $i = 1, \dots, n$ in the d -dimensional Euclidean space R^d , the multivariate kernel density estimate obtained with kernel $K(x)$ and window radius h , computed in the point x is defined as:

$$f(x) = \frac{1}{nh^d} \sum_{i=1}^n K\left(\frac{x-x_i}{h}\right) \quad (1)$$

Without loss of generality, let's assume $h = 1$ from now on, so we could simplify Equation (1) as:

$$f(x) = \frac{1}{n} \sum_{i=1}^n K(x-x_i) \quad (2)$$

$K(x)$ is generally a spherically symmetric kernel function satisfying:

$$K(x) = C_{k,d} k(\|x\|^2), \quad (3)$$

where $k(x)$ is the profile function of the kernel $K(x)$. $C_{k,d}$ is the normalizing constant such that

$$K(x) \geq 0, \quad (4)$$

and

$$\int_{R^d} K(x) dx = 1, \quad (5)$$

$\|x\|$ is the L_2 norm (i.e. Euclidean distance metric) of the d -dimensional vector x . Employing the profile function notation, Equation (2) can be further rewritten as

$$f(x) = \frac{C_{k,d}}{n} \sum_{i=1}^n k(\|x - x_i\|^2) \quad (6)$$

There are three types of commonly used spherical kernel functions $K(x)$: the Epanechnikov kernel, the uniform kernel, and the Gaussian kernel. The Epanechnikov kernel is defined by the profile function $k_E(x)$:

$$k_E(x) = \begin{cases} 1-x & 0 \leq x \leq 1 \\ 0 & x > 1 \end{cases} \quad (7)$$

The uniform kernel is defined by the profile function $k_U(x)$:

$$k_U(x) = \begin{cases} 1 & 0 \leq x \leq 1 \\ 0 & x > 1 \end{cases} \quad (8)$$

The Gaussian kernel is defined by the profile function $k_N(x)$:

$$k_N(x) = \exp\left(-\frac{1}{2}x\right) \quad x \geq 0 \quad (9)$$

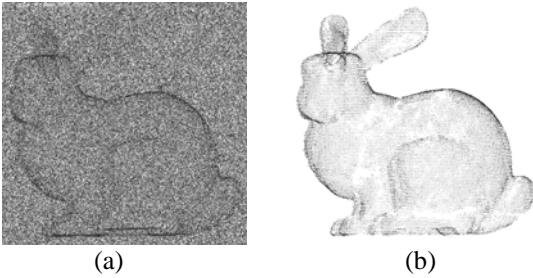
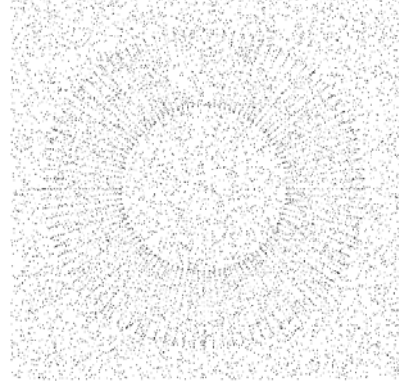
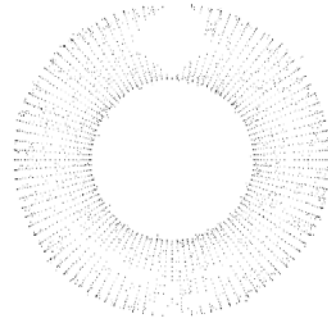


Figure 1: (a) The Stanford bunny (35678 points) with 1000% noise points added in; (b) Result after outlier removal.



(a)



(b)

Figure 2: (a) A synthetic torus point data (4800 points) which has an open hole in top, with 1000% noise points added in; (b) Result after outlier removal.

2.2 Outlier removal by anisotropic ellipsoidal kernel

For 3D point cloud obtained by laser scan or stereo vision, the outliers tend to spread in the space randomly, while “real” (we use a quotation here to emphasize the fact that the real surface is unknown) surface points will spread along a thin shell which encloses the real surface object. In other words, the distribution of the outliers is relatively isotropic, while the distribution of the real surface points is rather anisotropic. Hence in this paper, we propose to employ an anisotropic ellipsoidal kernel based density estimation method for outlier removal.

For anisotropic kernel, the L_2 norm $\|x-x_i\|$ in Equation (6), which measures the Euclidean distance metric between two points x and x_i will be replaced by the Mahalanobis distance metric $\|x-x_i\|_M$:

$$\|x-x_i\|_M = ((x-x_i)^t H^{-1} (x-x_i))^{1/2}, \quad (10)$$

here H is the covariance matrix defined as:

$$H = DD^T, \quad (11)$$

and

$$D = (x_1 - x, x_2 - x, \dots, x_n - x). \quad (12)$$

Geometrically, $(x - x_i)^t H^{-1} (x - x_i) = 1$ is a three-dimensional ellipsoid centered at x , with its shape and orientation defined by H . Using Single Value Decomposition (SVD), the covariance matrix H can be further decomposed as:

$$H = UAU^T, \quad (13)$$

with

$$A = \begin{bmatrix} \lambda_1 & 0 & 0 \\ 0 & \lambda_2 & 0 \\ 0 & 0 & \lambda_3 \end{bmatrix} \quad (14)$$

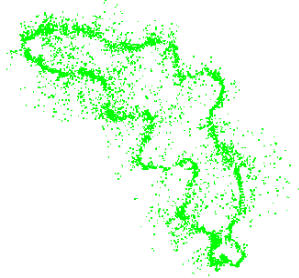
$\lambda_1 \geq \lambda_2 \geq \lambda_3$ are the three eigenvalues of the matrix H , and U is an orthonormal matrix whose columns are the eigenvectors of matrix H . We will detail the SVD-based decomposition (Equation (13)) of the covariance matrix H in the Appendix.

To compute the anisotropic kernel based density, we will apply an ellipsoidal kernel E of equal size and shape on all the data points. The orientation of the ellipsoidal kernel E will be determined locally. More specifically, given a point x , we will calculate its covariance matrix H by points located in its local spherical neighborhood of a fixed radius. Without loss of generality, we will assume the radius is 1 (which can be done by normalizing the data by the radius). The U matrix of Equation (13) calculated by the covariance analysis is kept unchanged to maintain the orientation of the ellipsoid. The size and shape of the ellipsoid will be modified to be the same as the ellipsoidal kernel E by modifying the diagonal matrix A as:

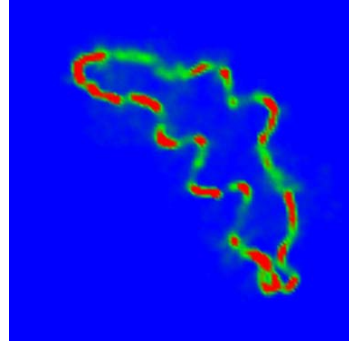
$$A = \begin{bmatrix} 1 & 0 & 0 \\ 0 & 1 & 0 \\ 0 & 0 & r \end{bmatrix}, \quad (15)$$

r is half of the length of the minimum axis of the ellipsoidal kernel E . After the density value is estimated, we will remove all the points whose estimated density value is smaller than a user-defined threshold. Figure 1 and Figure 2 are two examples of the proposed nonparametric density estimation based outlier removal from synthetic highly noisy data. The input of Figure 4 is a 3D point clouds obtained from multi-view stereo. Figure 4(a) is the original data; Figure 4(b) is the result after outlier removal. Figure 3 is a 2D slice view of the nonparametric data preprocessing process. In particular, Figure 3(a) is a 2D slice of the original 3D data of Figure 4(a); Figure

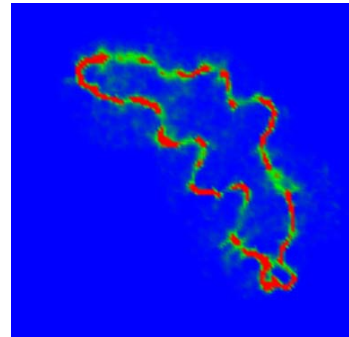
3(b) is the color-coded density map of Figure 3(a) estimated by an isotropic Gaussian kernel, with red represents the highest density and blue the lowest density; Figure 3(c) is the color-coded density map of Figure 3(a) estimated by an anisotropic Gaussian kernel of the same scale of Figure 3(b); Figure 3(d) is the result after outlier removal using Figure 3(b), and Figure 3(e) is the result after outlier removal using Figure 3(c). As we can see, better result is achieved by using the anisotropic kernel-based outlier removal (Figure 3(e)), comparing with the isotropic kernel-based outlier removal (Figure 3(d)).



(a)



(b)



(c)

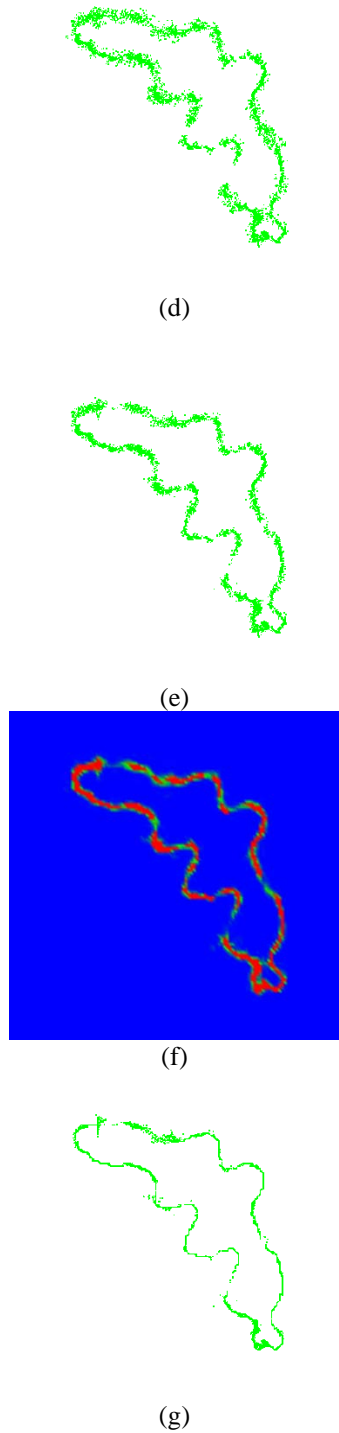
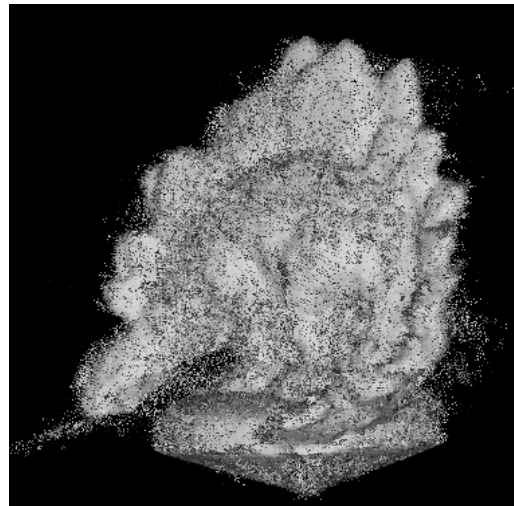


Figure 3: A 2D slice view of the nonparametric data preprocessing process. (a) a 2D slice of the original 3D data of Figure 4(a); (b) color-coded density map of (a) estimated by an isotropic Gaussian kernel, with red represents the highest density and blue the lowest density; (c) color-coded density map of (a) estimated

by an anisotropic Gaussian kernel of the same scale of (b); (d) after outlier removal using (b); (e) after outlier removal using (c); (f) color-coded density map of (e) estimated by an anisotropic Gaussian kernel of a smaller scale than (c); (g) result of projecting points of (e) by line search based on (f).

2.3 Point projection by line search

After the outlier removal step, we will need to further process the remaining point data so that they will be projected into the real surface. We will define the real surface as the set of points whose density value (estimated by the above Parzen-window based kernel density estimation) is maximum along its surface normal direction. This is similar to the concept of “extreme surface” as suggested by Amenta et al. [7]. We implement the data projection by a hill-climbing line search method. More specifically, given a point x , it will move along a direction l that is (approximately) orthogonal to the real surface, and will stop when a local maximum of the density value is reached. Since the real surface is unknown, the moving direction l is approximated by the eigenvector u_3 (Equation (21)) that is associated with the smallest eigenvalue σ_3^2 (Equation (21)) of the covariance matrix H (Equation (11)), calculated by the local neighbourhood of point x . The orientation of the moving direction is determined by the directional derivative of the density value along l , i.e. point x will always move uphill (i.e. move towards the direction that will increase the density value). Figure 4(c) shows the result of projecting data points by line search. A 2D slice view of the point projection is shown in Figure 3(g). Note that the outlier removal and the point projection procedure can be iterated one or two times to further improve the result.



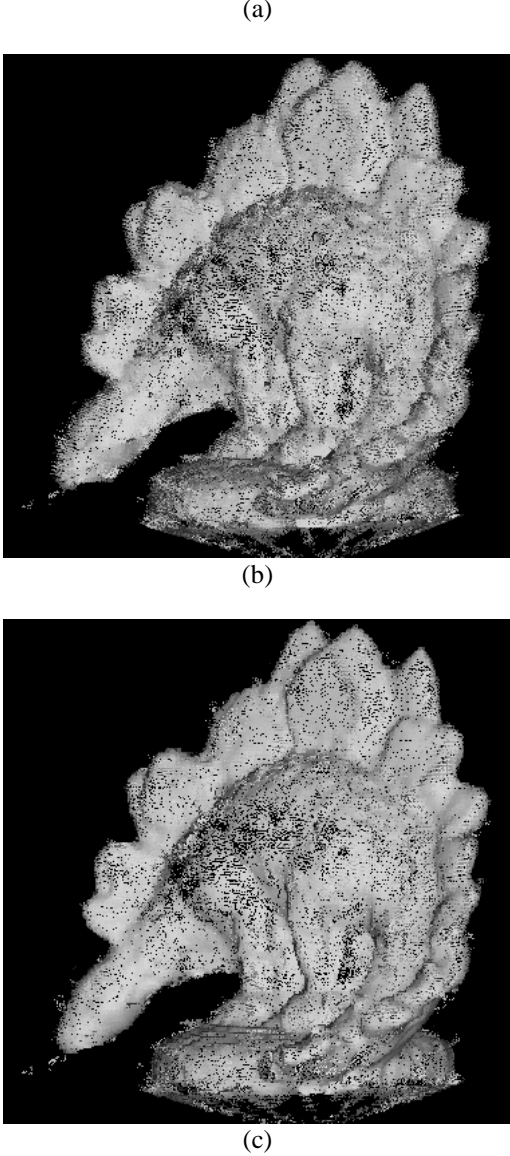


Figure 4: (a) 3D point clouds (660,000 points) obtained from multi-view stereo; (b) after outlier removal; (c) after point projection by line search.

3. Conclusions and Future Work

In this paper, we propose a nonparametric approach for noisy point data preprocessing. In particular, we proposed an anisotropic kernel based nonparametric density estimation for outlier removal, and a hill-climbing line search approach for projecting data points onto the real surface boundary. Our method is very robust with highly noisy dataset, as can be seen from the examples shown. In addition, our approach is computationally very efficient. For example, it only takes 3 to 4 minutes in a middle-range desktop PC to

process (outlier removal and point projection) the multi-view stereo point data (Figure 4) which contains more than 600,000 points. The majority of the running time actually spends on computing the density. The line search based projection is done in less than 10 seconds for the whole dataset.

The main limitation of our approach is that currently a fixed bandwidth of the kernel is used across the whole dataset, which can cause some of the “good” data being removed during the outlier removal process (as can be seen in Figure 3(e)). We would like to develop a scheme that can automatically select the optimal kernel bandwidth based on the local neighborhood. We would also like to extend our approach so that it can handle hole fillings automatically.

4. Acknowledgments

We are very grateful to the Stanford Graphics Archive for the bunny dataset, and to Steve Seitz et al. [1] for the multi-view stereo image datasets.

5. Appendix: Decomposition of the Covariance Matrix H

Since the covariance matrix H is defined as:

$$H = DD^T,$$

and

$$D = (x_1 - x, x_2 - x, \dots, x_n - x).$$

Using Single Value Decomposition (SVD), D can be decomposed as:

$$D = U\Sigma V^T \quad (16)$$

Σ is the diagonal matrix:

$$\Sigma = \begin{bmatrix} \sigma_1 & 0 & 0 \\ 0 & \sigma_2 & 0 \\ 0 & 0 & \sigma_3 \end{bmatrix}, \quad (17)$$

with $\sigma_1 \geq \sigma_2 \geq \sigma_3$. U and V are orthonormal matrixes, i.e. $U^T U = V^T V = I$, I is the identity matrix. So,

$$H = DD^T = U\Sigma V^T V\Sigma U^T = U\Sigma^2 U^T, \quad (18)$$

and let's define matrix A as:

$$A = \Sigma^2, \quad (19)$$

which is also a diagonal matrix. Thus we have

$$H = UAU^T. \quad (20)$$

Furthermore, if we denote $U = (u_1, u_2, u_3)$, since U is an orthonormal matrix, we will have

$$Hu_i = \sigma_i^2 u_i, \quad (21)$$

which means u_i is the eigenvector of H , associated with its i^{th} largest eigenvalue σ_i^2 .

6. References

- [1] Steve Seitz, Brian Curless, James Diebel, Daniel Scharstein, Richard Szeliski, A Comparison and Evaluation of Multi-View Stereo Reconstruction Algorithms, CVPR 2006, vol. 1, pages 519-526.
- [2] N. Amenta and M. Bern, Surface reconstruction by voronoi filtering, *Discrete and Comput. Geometry*, vol. 22, pp. 481-504, 1999.
- [3] H. Edelsbrunner, Shape reconstruction with delaunay complex, in *LATIN '98: Proceedings of the Third Latin American Symposium on Theoretical Informatics*, (London, UK), pp. 119-132, Springer-Verlag, 1998.
- [4] J. D. Boissonnat, Geometric structures for three dimensional shape reconstruction, *ACM Trans. Graphics* 3, pp. 266-286, 1984.
- [5] N. Amenta, M. Bern, and D. Eppstein, The crust and the -skeleton: Combinational curve reconstruction, 14th ACM Symposium on Computational Geometry, 1998.
- [6] N. Amenta, M. Bern, and M. Kamvysselis, A new voronoi-based surface reconstruction algorithm, in *SIGGRAPH '98: Proceedings of the 25th annual conference on Computer graphics and interactive techniques*, (New York, NY, USA), pp. 415-421, ACM Press, 1998.
- [7] Nina Amenta, Yong Joo Kil: Defining point-set surfaces. *ACM Trans. Graph.* 23(3): 264-270 (2004)
- [8] G. Medioni, M.-S. Lee, and C.-K. Tang, A computational framework for segmentation and grouping. Elsevier, 2000.
- [9] Richard O. Duda Peter E. Hart David G. Stork, *Pattern Classification*, October 2000, Wiley-Interscience; 2 edition.
- [10] H. Hoppe, T. DeRose, T. Duchamp, J. McDonald, and W. Stuetzle, Surface reconstruction from unorganized points, in *SIGGRAPH '92: Proceedings of the 19th annual conference on Computer graphics and interactive techniques*, (New York, NY, USA), pp. 71-78, ACM Press, 1992.
- [11] C. L. Bajaj, F. Bernardini, and G. Xu, Automatic reconstruction of surfaces and scalar fields from 3d scans, in *SIGGRAPH '95: Proceedings of the 22nd annual conference on Computer graphics and interactive techniques*, (New York, NY, USA), pp. 109-118, ACM Press, 1995.
- [12] B. Curless and M. Levoy, A volumetric method for building complex models from range images, in *SIGGRAPH '96: Proceedings of the 23rd annual conference on Computer graphics and interactive techniques*, (New York, NY, USA), pp. 303-312, ACM Press, 1996.
- [13] A. Hilton, A. J. Stoddart, J. Illingworth, and T. Winder, Implicit surface-based geometric fusion, *Comput. Vis. Image Underst.*, vol. 69, no. 3, pp. 273-291, 1998.
- [14] R. Whitaker, A level set approach to 3D reconstruction from range data, *International journal of Computer Vision*, 1997.
- [15] H.-K. Zhao, S. Osher, B. Merriman, and M. Kang, Implicit and non-parametric shape reconstruction from unorganized data using a variational level set method, *Computer Vision and Image Understanding*, vol. 80, pp. 295-319, 2000.
- [16] H. Zhao, S. Osher, and R. Fedkiw, Fast surface reconstruction using the level set method, in *VLSM '01: Proceedings of the IEEE Workshop on Variational and Level Set Methods (VLSM'01)*, (Washington, DC, USA), p. 194, IEEE Computer Society, 2001.
- [17] J. C. Carr, R. K. Beatson, J. B. Cherrie, T. J. Mitchell, W. R. Fright, B. C. McCallum, and T. R. Evans, Reconstruction and representation of 3d objects with radial basis functions, in *SIGGRAPH '01: Proceedings of the 28th annual conference on Computer graphics and interactive techniques*, (New York, NY, USA), pp. 67-76, ACM Press, 2001.
- [18] Y. Ohtake, A. Belyaev, M. Alexa, G. Turk, and H. Seidel, Multi-level partition of unity implicits, *ACM Trans. Graph.* 2003, Pages: 463-470.
- [19] H. Xie, J. Wang, J. Hua, H. Qin, and A. Kaufman, Piecewise c1 continuous surface reconstruction of noisy point clouds via local implicit quadric regression. *IEEE Visualization 2003*, 91-98.
- [20] D. Levin. 2003. Mesh-independent surface interpolation. In *Geometric Modeling for Scientific Visualization*, G. Brunnert, B. Hamann, K. Mueller, and L. Linsen, Eds. Springer-Verlag.
- [21] M. Alexa, J. Behr, D. Cohen-Or, S. Fleishman, D. Levin, and C. T. Silva. Computing and rendering point set surfaces. *IEEE Transactions on Visualization and Computer Graphics* 9, 1, 3-15. 2003.